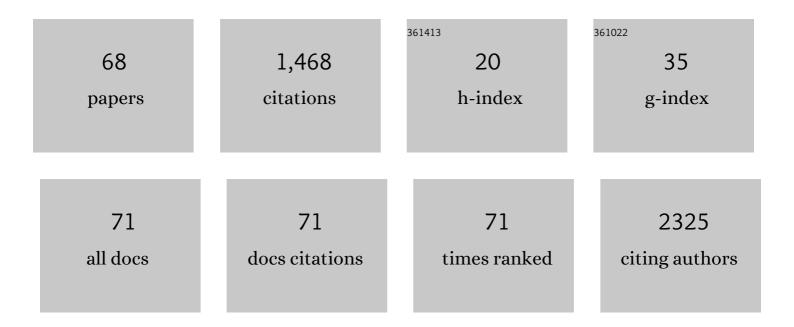
Andreas Pohlmann

List of Publications by Year in descending order

Source: https://exaly.com/author-pdf/6497624/publications.pdf Version: 2024-02-01



#	Article	IF	CITATIONS
1	Toll-like receptor 2 mediates microglia/brain macrophage MT1-MMP expression and glioma expansion. Neuro-Oncology, 2013, 15, 1457-1468.	1.2	115
2	How bold is blood oxygenation levelâ€dependent (BOLD) magnetic resonance imaging of the kidney? Opportunities, challenges and future directions. Acta Physiologica, 2015, 213, 19-38.	3.8	100
3	Longitudinal regional brain volume changes quantified in normal aging and Alzheimer's APP×PS1 mice using MRI. Brain Research, 2009, 1270, 19-32.	2.2	97
4	GDNF mediates glioblastoma-induced microglia attraction but not astrogliosis. Acta Neuropathologica, 2013, 125, 609-620.	7.7	97
5	Detailing the Relation Between Renal T2* and Renal Tissue pO2 Using an Integrated Approach of Parametric Magnetic Resonance Imaging and Invasive Physiological Measurements. Investigative Radiology, 2014, 49, 547-560.	6.2	64
6	Claudin peptidomimetics modulate tissue barriers for enhanced drug delivery. Annals of the New York Academy of Sciences, 2017, 1397, 169-184.	3.8	58
7	Rectal cancer: Assessment of response to neoadjuvant chemoradiation by dynamic contrast-enhanced MRI. Journal of Magnetic Resonance Imaging, 2013, 38, 119-126.	3.4	52
8	High Temporal Resolution Parametric MRI Monitoring of the Initial Ischemia/Reperfusion Phase in Experimental Acute Kidney Injury. PLoS ONE, 2013, 8, e57411.	2.5	51
9	Technical recommendations for clinical translation of renal MRI: a consensus project of the Cooperation in Science and Technology Action PARENCHIMA. Magnetic Resonance Materials in Physics, Biology, and Medicine, 2020, 33, 131-140.	2.0	44
10	Visualizing Brain Inflammation with a Shingled-Leg Radio-Frequency Head Probe for 19F/1H MRI. Scientific Reports, 2013, 3, 1280.	3.3	39
11	Assessment of tumor microcirculation with dynamic contrastâ€enhanced MRI in patients with esophageal cancer: Initial experience. Journal of Magnetic Resonance Imaging, 2008, 27, 1296-1301.	3.4	37
12	Linking nonâ€invasive parametric <scp>MRI</scp> with invasive physiological measurements (<scp>MR</scp> â€ <scp>PHYSIOL</scp>): towards a hybrid and integrated approach for investigation of acute kidney injury in rats. Acta Physiologica, 2013, 207, 673-689.	3.8	35
13	Advancing Cardiovascular, Neurovascular, and Renal Magnetic Resonance Imaging in Small Rodents Using Cryogenic Radiofrequency Coil Technology. Frontiers in Pharmacology, 2015, 6, 255.	3.5	35
14	Enhanced Fluorine-19 MRI Sensitivity using a Cryogenic Radiofrequency Probe: Technical Developments and Ex Vivo Demonstration in a Mouse Model of Neuroinflammation. Scientific Reports, 2017, 7, 9808.	3.3	34
15	Functional and Morphological Cardiac Magnetic Resonance Imaging of Mice Using a Cryogenic Quadrature Radiofrequency Coil. PLoS ONE, 2012, 7, e42383.	2.5	32
16	Identification of Cellular Infiltrates during Early Stages of Brain Inflammation with Magnetic Resonance Microscopy. PLoS ONE, 2012, 7, e32796.	2.5	30
17	Early effects of an xâ€ray contrast medium on renal T ₂ */T ₂ ×scp>MRI as compared to shortâ€term hyperoxia, hypoxia and aortic occlusion in rats. Acta Physiologica, 2013, 208, 202-213.	3.8	29
18	A synthetic epoxyeicosatrienoic acid analogue prevents the initiation of ischemic acute kidney injury. Acta Physiologica, 2019, 227, e13297.	3.8	26

ANDREAS POHLMANN

#	Article	IF	CITATIONS
19	Diffusion-Sensitized Ophthalmic Magnetic Resonance Imaging Free of Geometric Distortion at 3.0 and 7.0 T. Investigative Radiology, 2015, 50, 309-321.	6.2	24
20	Enlargement of Cerebral Ventricles as an Early Indicator of Encephalomyelitis. PLoS ONE, 2013, 8, e72841.	2.5	22
21	Magnetic resonance safety and compatibility of tantalum markers used in proton beam therapy for intraocular tumors: A 7.0 Tesla study. Magnetic Resonance in Medicine, 2017, 78, 1533-1546.	3.0	21
22	Myocardial effective transverse relaxation time T2* Correlates with left ventricular wall thickness: A 7.0 T MRI study. Magnetic Resonance in Medicine, 2017, 77, 2381-2389.	3.0	21
23	Somatosensory BOLD fMRI reveals close link between salient blood pressure changes and the murine neuromatrix. Neurolmage, 2018, 172, 562-574.	4.2	21
24	MRI of tarantulas: morphological and perfusion imaging. Magnetic Resonance Imaging, 2007, 25, 129-135.	1.8	19
25	Cardiomyocyte-derived CXCL12 is not involved in cardiogenesis but plays a crucial role in myocardial infarction. Journal of Molecular Medicine, 2016, 94, 1005-1014.	3.9	18
26	Assessment of Blood Brain Barrier Leakage with Gadolinium-Enhanced MRI. Methods in Molecular Biology, 2018, 1718, 395-408.	0.9	18
27	Antibodies to the α1-Adrenergic Receptor Cause Vascular Impairments in Rat Brain as Demonstrated by Magnetic Resonance Angiography. PLoS ONE, 2012, 7, e41602.	2.5	18
28	Anatomic and pathological characterization of choroidal melanoma using multimodal imaging. Melanoma Research, 2015, 25, 252-258.	1.2	17
29	Progression and variability of TNBS colitis-associated inflammation in rats assessed by contrast-enhanced and T2-weighted MRI. Inflammatory Bowel Diseases, 2009, 15, 534-545.	1.9	16
30	Fluorine-19 MRI at 21.1ÂT: enhanced spin–lattice relaxation of perfluoro-15-crown-5-ether and sensitivity as demonstrated in ex vivo murine neuroinflammation. Magnetic Resonance Materials in Physics, Biology, and Medicine, 2019, 32, 37-49.	2.0	16
31	Probing renal blood volume with magnetic resonance imaging. Acta Physiologica, 2020, 228, e13435.	3.8	16
32	Experimental MRI Monitoring of Renal Blood Volume Fraction Variations En Route to Renal Magnetic Resonance Oximetry. Tomography, 2017, 3, 188-200.	1.8	16
33	Anchoring Dipalmitoyl Phosphoethanolamine to Nanoparticles Boosts Cellular Uptake and Fluorine-19 Magnetic Resonance Signal. Scientific Reports, 2015, 5, 8427.	3.3	15
34	Normothermic Mouse Functional MRI of Acute Focal Thermostimulation for Probing Nociception. Scientific Reports, 2016, 6, 17230.	3.3	15
35	Effect of changes in lung volume on acoustic transmission through the human respiratory system. Physiological Measurement, 2001, 22, 233-243.	2.1	14
36	Cerebral blood volume estimation by ferumoxytol-enhanced steady-state MRI at 9.4 T reveals microvascular impact of α1 -adrenergic receptor antibodies. NMR in Biomedicine, 2014, 27, 1085-1093.	2.8	14

ANDREAS POHLMANN

#	Article	IF	CITATIONS
37	Performance of compressed sensing for fluorineâ€19 magnetic resonance imaging at low signalâ€toâ€noise ratio conditions. Magnetic Resonance in Medicine, 2020, 84, 592-608.	3.0	14
38	Transient enlargement of brain ventricles during relapsing-remitting multiple sclerosis and experimental autoimmune encephalomyelitis. JCI Insight, 2020, 5, .	5.0	13
39	Acute effects of ferumoxytol on regulation of renal hemodynamics and oxygenation. Scientific Reports, 2016, 6, 29965.	3.3	12
40	Monitoring Dendritic Cell Migration using ¹⁹ F / ¹ H Magnetic Resonance Imaging. Journal of Visualized Experiments, 2013, , e50251.	0.3	11
41	Continuous diffusion spectrum computation for diffusion-weighted magnetic resonance imaging of the kidney tubule system. Quantitative Imaging in Medicine and Surgery, 2021, 11, 3098-3119.	2.0	11
42	<i>In vivo</i> detection of teriflunomide-derived fluorine signal during neuroinflammation using fluorine MR spectroscopy. Theranostics, 2021, 11, 2490-2504.	10.0	10
43	Magnetic Resonance Imaging (MRI) Analysis of Ischemia/Reperfusion in Experimental Acute Renal Injury. Methods in Molecular Biology, 2016, 1397, 113-127.	0.9	10
44	Assessment of Renal Hemodynamics and Oxygenation by Simultaneous Magnetic Resonance Imaging (MRI) and Quantitative Invasive Physiological Measurements. Methods in Molecular Biology, 2016, 1397, 129-154.	0.9	9
45	ERK1 as a Therapeutic Target for Dendritic Cell Vaccination against High-Grade Gliomas. Molecular Cancer Therapeutics, 2016, 15, 1975-1987.	4.1	7
46	Myocardial Effective Transverse Relaxation Time T 2 * is Elevated in Hypertrophic Cardiomyopathy: A 7.0 T Magnetic Resonance Imaging Study. Scientific Reports, 2018, 8, 3974.	3.3	7
47	Reliable kidney size determination by magnetic resonance imaging in pathophysiological settings. Acta Physiologica, 2021, 233, e13701.	3.8	7
48	Functional Imaging Using Fluorine (19F) MR Methods: Basic Concepts. Methods in Molecular Biology, 2021, 2216, 279-299.	0.9	6
49	Pharmacological fMRI - Challenges in Analysing Drug-Induced Single-Event BOLD Responses. Annual International Conference of the IEEE Engineering in Medicine and Biology Society, 2007, 2007, 3411-6.	0.5	5
50	Cardiac MRI in Small Animals. Methods in Molecular Biology, 2018, 1718, 269-284.	0.9	5
51	B ₁ inhomogeneity correction of RARE MRI with transceive surface radiofrequency probes. Magnetic Resonance in Medicine, 2020, 84, 2684-2701.	3.0	5
52	B ₁ inhomogeneity correction of RARE MRI at low SNR: Quantitative in vivo ¹⁹ F MRI of mouse neuroinflammation with a cryogenically ooled transceive surface radiofrequency probe. Magnetic Resonance in Medicine, 2022, 87, 1952-1970.	3.0	5
53	Diffusion-weighted Renal MRI at 9.4 Tesla Using RARE to Improve Anatomical Integrity. Scientific Reports, 2019, 9, 19723.	3.3	4
54	Monitoring Renal Hemodynamics and Oxygenation by Invasive Probes: Experimental Protocol. Methods in Molecular Biology, 2021, 2216, 327-347.	0.9	4

#	Article	IF	CITATIONS
55	Recommendations for Preclinical Renal MRI: A Comprehensive Open-Access Protocol Collection to Improve Training, Reproducibility, and Comparability of Studies. Methods in Molecular Biology, 2021, 2216, 3-23.	0.9	3
56	Cardiovascular magnetic resonance detects microvascular dysfunction in a mouse model of hypertrophic cardiomyopathy. Journal of Cardiovascular Magnetic Resonance, 2021, 23, 63.	3.3	3
57	Interpretation of functional renal MRI findings: Where physiology and imaging sciences need to talk across domains. Journal of Magnetic Resonance Imaging, 2018, 47, 1140-1141.	3.4	2
58	Cardiorenal sodium MRI in small rodents using a quadrature birdcage volume resonator at 9.4ÂT. Magnetic Resonance Materials in Physics, Biology, and Medicine, 2020, 33, 121-130.	2.0	2
59	Physiological system analysis of the kidney by highâ€ŧemporalâ€ෑesolution monitoring of an oxygenation step response. Magnetic Resonance in Medicine, 2021, 85, 334-345.	3.0	2
60	Tissue optical properties from spatially resolved reflectance: calibration and in vivo application on rat kidney. Proceedings of SPIE, 2017, , .	0.8	2
61	Hardware Considerations for Preclinical Magnetic Resonance of the Kidney. Methods in Molecular Biology, 2021, 2216, 131-155.	0.9	1
62	Fluorine (19F) MRI for Assessing Inflammatory Cells in the Kidney: Experimental Protocol. Methods in Molecular Biology, 2021, 2216, 495-507.	0.9	1
63	Subsegmentation of the Kidney in Experimental MR Images Using Morphology-Based Regions-of-Interest or Multiple-Layer Concentric Objects. Methods in Molecular Biology, 2021, 2216, 549-564.	0.9	1
64	Analysis Protocols for MRI Mapping of the Blood Oxygenation–Sensitive Parameters T2* and T2 in the Kidney. Methods in Molecular Biology, 2021, 2216, 591-610.	0.9	1
65	Denoising for Improved Parametric MRI of the Kidney: Protocol for Nonlocal Means Filtering. Methods in Molecular Biology, 2021, 2216, 565-576.	0.9	1
66	Reliable determination of tissue optical properties from spatially resolved reflectance. Proceedings of SPIE, 2017, , .	0.8	0
67	Renal MRI Diffusion: Experimental Protocol. Methods in Molecular Biology, 2021, 2216, 419-428.	0.9	0
68	Near Infrared Spectroscopy Setup for Concurrent Spectroscopic, Invasive and MRI Investigations in		0

⁶⁸ Rats., 2018, , .